Inversion of Spectral Absorption in the Optically Complex Coastal Waters of the Mid-Atlantic Bight

Oscar Schofield, Trisha Bergmann, Mathew J. Oliver, and Andrew Irwin
Coastal Ocean Observation Laboratory, Institute of Marine and Coastal Sciences
Rutgers University, New Brunswick, NJ 08901

Gary Kirkpatrick
Mote Marine Laboratory, 1600 Ken Thompson Parkway
Sarasota, FL., 34236

Paul W. Bissett
Florida Environmental Research Institute, 4807 Bayshore Blvd. Suite 101,
Tampa, FL 33611

Mark A. Moline and Cris Orrico
Biological Sciences Department, California Polytechnic State University,
San Luis Obispo, CA 93407

Keywords: Absorption, Phytoplankton, Bio-Optics, Water Mass Analysis

Running Title: Inversion of Bulk Optics

Abstract

Recent advances in hydrologic optics offer the potential for quantitative maps of inherent optical properties, which can be inverted into optically significant constituents. During summer experiments in the Mid-Atlantic Bight (MAB) a procedure to invert bulk absorption measurements from off-the-shelf technology was developed. The inversion provides optical concentration estimates of phytoplankton, colored dissolved organic matter (CDOM), and detritus. Inversion estimates were validated against chlorophyll fluorescence, filter pad absorption, and phytoplankton pigment measurements. The inversion could account for up to 90% of the observed variance in particulates, CDOM, and detritus. Robust estimates for phytoplankton community composition could be achieved but required constraints on the inversion that phytoplankton dominate the red light absorption. Estimates for the composition, as indicated by spectral slopes, for CDOM and detritus were not robust. During the summer months in nearshore waters of the MAB total absorption was almost equally associated ($\pm$10%) with phytoplankton, detritus, and CDOM and the regions of variability were associated with major frontal boundaries. The variance between particulates, CDOM and detritus varied spatially and with year; which precluded robust correlations.

1. Introduction

Traditional “conservative” parameters (e.g. temperature and salinity) have been used to track water masses for nearly a century (Helland-Hansen 1916) but developing additional parameters from chemical signatures to extend water type identification and water mass analysis into multi-dimensional space is of great utility (Tomczak 1999). Such a capability would improve adaptive sampling strategies (Robinson and Glenn 1999), allowing researchers to study how water masses evolve and optimize sampling strategies.

It has been suggested that traditional water mass markers might be complemented with standard biological measurements such as chlorophyll (Tomczak 1999) as an additional dimension would improve resolving water types in parameter space. Chlorophyll is a logical choice for this additional discrimination dimension, as it is the pre-eminent proxy for phytoplankton abundance and can be estimated relatively easily by satellites and *in situ* sensors. Fluorometry is a powerful *in situ* mapping approach, however variability in the fluorescence quantum yields requires local calibration data for deriving any quantitative estimate. This is difficult as changes in the fluorescence quantum yield reflect sensitivities to both the incident spectral irradiance and overall phytoplankton physiology (Kiefer 1973, Cullen 1982, Falkowski and Kiefer 1985), both of which can change on the time scale of hours to days (cf. Falkowski and Raven 1997).

Another potential variable might be Colored Dissolved Organic Matter (CDOM), which has been used successfully to calibrate mass transport (Aarup et al. 1996, Højerslev et al. 1996). Most coastal systems reflect the optical contributions of numerous in-water constituents [water, phytoplankton, CDOM, detritus, and sediment]. This

optical complexity compromises the accuracy of the satellite-derived products (cf. Kirk 1995, Mobley 1995); however this complex matrix of materials provides a potential library of parameters that might be effective for discriminating water types if methods could be developed that provide reliable estimates of the optically-significant constituents present.

Significant effort over the last decade has focused on measuring the spectral dependency of the *in situ* inherent optical properties (IOPs). The reliability *in situ* instrumentation that can measure the spectral IOPs is increasing (Pegau et al. 1995, Twardowksi et al. 1999, Chang and Dickey 1999, Schofield et al. 1999, Boss et al. 2001). A major advantage of these parameters is that they can be inverted to provide weights for optically active components [e.g. water, colored dissolved organic matter (CDOM), phytoplankton, detritus, sediment, etc.]. These optical weights are proportional to component concentration (Roesler and Perry 1995, Chang and Dickey 1999, Schofield et al. 1999, Gallegos and Neale 2002). These inversion techniques are often based on estimating the total absorption using generalized spectral absorption shapes for one or more of the individual absorbing components or using absorption ratios of different wavelengths that vary in a predictable way according to the components present. While promising in theory, the accuracy of these inverted measurements have not been systematically assessed over the wide optical gradients present in the nearshore coastal ocean. Furthermore, the performance of inversion techniques that do not require any "optimized" local *in situ* data to derive the generalized shapes has yet to be assessed. Ideally, minimal "local" tuning should be applied to these inversion techniques as this would allow for a "global" mechanistic approach, which is particularly important in

complex coastal waters where local empirical relationships are likely to be extremely variable.

In this manuscript, we assess the application of a simple optical inversion method using off-the-shelf oceanographic equipment for deriving optical parameters, and assess the utility of the derived optical parameters to differentiate water types in the coastal ocean. Our goal is to assess how much information can be inverted from absorption data given a fixed number of wavelengths, which can then be used to determine the "optical" state of nearshore coastal waters.

2. Methods

2.1 Field Data

The field efforts were conducted at the Long term Ecosystem Observatory (LEO) off the central coast of New Jersey (Glenn et al. 1998, Glenn et al. 2000, Schofield et al. 2002) during the ONR-sponsored Hyperspectral Coastal Ocean Dynamics Experiments (HyCODE) and the Coastal Ocean Modeling and Observation Program (COMOP). The LEO system is a highly instrumented 30 by 30 km research site that represents a coupled model/observation system where real-time data and model forecasts are provided to optimize field sampling (Glenn et al. 1998, Schofield et al. 2002). For bio-optical research, one advantage of the field site is that it ranges from very turbid estuarine waters to relatively clear offshore waters within the 30 km research box. These optical gradients reflect the variable contributions of many optically-active constituents such as phytoplankton, sediments, CDOM, and detritus.

The standard shipboard surveys consisted of several 15-25 km cross-shelf transects. Specific transect lines and the locations of the stations were determined by the

real-time data from ocean forecast models, other ships and satellites (Schofield et al. 2002). At each station, vertical profiles of optical and physical data were collected using an integrated bio-optical package. The bio-optical package consisted of a WET Labs Inc. absorption/attenuation meter (ac-9), a Falmouth CTD, a profiling Satlantic spectral radiometer, and a HOBI Labs backscatter sensor (Hydroscat-6). The measurements of the inherent optical properties used in this study were collected using the standard nine-wavelengths (412, 440, 488, 510, 555, 630, 650, 676, 715 nm) of the WET Labs Inc. ac-9. At each station, the instrument was lowered to depth to remove air bubbles and the instrument was allowed to equilibrate with ambient temperature before data were collected. Only data from the upcasts were utilized. Data were averaged into 0.25-meter depth bins for all subsequent analyses. The instruments were factory calibrated prior to the field seasons. Manufacturer recommended protocols (http://www.WET Labs Inc..com/otherinfo/ugftp.htm) were used to track instrument calibration throughout the field season. This included clean water, temperature, and salinity calibrations. Whenever possible daily water calibrations were conducted; however sampling schedules did not always allow for a daily calibration. Under these circumstances the most recent water calibration was used. It should be noted that this period without a calibration was at most three days.

A CDOM absorption mapping system was installed on the ship (Kirkpatrick et al. 2003), which consisted of a liquid-waveguide capillary cell (LWCC, World Precision Instruments, Inc.) coupled to a fiber-optic spectrometer (S2000, Ocean Optics, Inc.) and a fiber-optic xenon flashlamp (PS-2, Ocean Optics, Inc.). Water was pumped by miniature peristaltic pump (P625, Instech Laboratories, Inc.) through size-fractionation and cross-

flow filters (MicroKros, Spectrum Laboratories, Inc.) and then through the LWCC for optical density spectra measurements. A continuous underway water supply was provided by tapping the flow through the ship's fire suppression system. Details regarding the LWCC operation procedures can be found in Kirkpatrick et al. (2003).

At each ship occupied station, water was collected with Niskin bottles from both surface and bottom waters. Aliquots were filtered, under low vacuum (<10 cm Hg), through GF/F (Whatman) glass-fiber filters to concentrate the particles for pigment and absorption determinations. Filters were placed into snap top vials and quick frozen in liquid nitrogen. Samples were stored at –80 ˚C until later analysis. Filters were analyzed for photosynthetic and photoprotective pigment complements using high-performance liquid chromatography (HPLC) according to procedures of Wright et al. (1991). Filter pad absorption was measured on a laboratory spectrophotometer; spectra were corrected for the pathlength amplification factor according to the procedures outlined in Roesler (1998). Detrital absorption was determined by methanol extraction of particulate material according to Kishino et al. (1985). The detrital absorption was subtracted from particulate absorption to provide an estimate of phytoplankton absorption. For discrete CDOM spectra, water was filtered through a 0.2 micron Nucleopore filter, and measured on a spectrophotometer using a 5 cm long path length cuvette.

A second *in situ* data set was collected using a bottom mounted winch that profiled an instrument package. The Optical Profiler contained a WET Labs ac-9 sampling at 6 Hz, and a two-wavelength backscatter/fluorometer HOBI Labs HydroScat-2 sampling at 2 Hz. The Optical Profiler was profiled at 2 cm s^{-1}. The profiler was connected to the electro-fiber optic LEO cable, allowing real-time data transmission back

to shore. A detailed description of this system is provided in Oliver et al. (2004b). This data set was complemented with a radioisotope dataset (cf. Oliver et al. 2004) and that allowed us to assess the proportion of the water that was light saturated for photosynthesis.

2.2 Inversion of *in situ* absorption data

The optical signature inversion method (OSI) uses measured spectral absorption data collected from the ac-9 to calculate optical weight specific absorption coefficients for material present in the water column. The OSI model calculates optical weight specific coefficients (w_i) and exponential slopes (*s, r*) using a non-linear constrained least-squares regression according to

$$a_{total}(\lambda) = w_1 a_{Phyto1}(\lambda) + w_2 a_{Phyto2}(\lambda) + w_3 a_{Phyto3}(\lambda) + w_4 a_{CDOM}(\lambda, s) + w_5 a_{Detritus}(\lambda, r) \quad (1)$$

where $a_{total}(\lambda)$ is the total spectral absorption measured with the ac-9 (note that ac-9 provides absorption that has already subtracted the contribution due to water), $a_{Phyto1}(\lambda)$, $a_{Phyto2}(\lambda)$ and $a_{Phyto3}(\lambda)$ are generalized spectral absorption of chlorophyll *a-c*, phycobilin and chlorophyll *a-b* containing phytoplankton respectively, and $a_{CDOM}(\lambda, s)$ and $a_{Detritus}(\lambda, r)$ are the spectral absorption of CDOM and detritus (Fig. 1). The CDOM absorption (and detritus absorption) can be described as an idealized curve as a function of wavelength and exponential slope (Kalle 1966, Bricaud et al. 1981, Green and Blough 1994),

$$a_{CDOM}(\lambda) = a_{CDOM} \exp[-s \bullet (\lambda - 412nm)] \quad (2)$$

The exponential *s* parameter (unitless) is dependent on the composition of the CDOM present and is highly variable (Carder et al. 1989, Roesler et al. 1989). Therefore, it was

necessary to allow the CDOM and detritus exponential slopes to vary spatially and temporally to achieve reasonable estimates. The initial exponential slopes of CDOM were set to 0.010. The detritus exponential slope was initially set to 0.008. The slopes of the detrital curves (*r*) are lower (cf. Kirk 1995) and detritus is described by Equation 3,

$$a_{Detritus}(\lambda) = a_{Detritus} \exp[-r \bullet (\lambda - 412nm)] \quad (3)$$

The values of w_1, w_2, w_3, w_4 and w_5 are non-spectrally dependent scalar coefficients of these input spectra. We used fixed absorption spectra measured on laboratory cultures in order to ensure that inversion was completely independent from any spectral curves encountered in the field. Spectral phytoplankton curves were of averages of high-light and low-light acclimated phytoplankton spectra that were normalized to absorption at 676 nm. The spectral library used was taken from Johnsen et al 1994 (Figure 1). While not optimal, we believe it was reasonable since the first order determinant of spectral optical signals reflects the overall concentration of material rather then spectral characteristics of the materials present (Barnard et al. 1998).

We used two different inversion approaches, one with more constraints than the other. The minimal constraint OSI (OSI_m) only required that all solutions be positive (Eqn. 4), that CDOM and detritus absorption weights were equal in the red wavelengths of light (Eqn. 5), and that the CDOM exponential slope is steeper than the detrital slope (Eqn. 6). The assumption that the CDOM and detritus absorption is equal is artificial but we know that CDOM and detritus absorption is very low in the red wavelengths as both are exponentially decreasing curves. There are two artificial ways to ensure that the CDOM and detritus absorption do not dominate the red light absorption where phytoplankton absorption dominates. One method, more commonly used, is to set the

magnitude of CDOM and detritus red absorption to a fixed low value. The second method is to anchor both curves to each other in the red which allows the exponential slopes and amplitudes to be determined largely by the blue wavelength absorption. This second method allows the red light absorption of CDOM and detritus to be variable. The second OSI method (OSI_c) added constraints so that phytoplankton absorption explicitly dominated in the red wavelengths (Eqns 7 and 8), and that minor phytoplankton communities in these waters (here chlorophytes) were never dominant (Eqns. 9 and 10). Specifically, the constraints on the OSI optimizations were:

$$w_1 a_{Phyto1}(\lambda), w_2 a_{Phyto2}(\lambda), w_3 a_{Phyto3}(\lambda), w_4 a_{CDOM}(\lambda, s), w_5 a_{Detritus}(\lambda, r) \geq 0 \quad (4)$$

$$w_4 a_{CDOM}(676nm, s) = w_5 a_{Detritus}(676nm, r) \quad (5)$$

$$s \geq r \quad (6)$$

$$w_1 a_{Phyto1}(676nm) \geq w_4 a_{CDOM}(676nm, s) + w_5 a_{Detritus}(676nm, r) \geq 0 \quad (7)$$

$$w_2 a_{Phyto2}(676nm) \geq w_4 a_{CDOM}(676nm, s) + w_5 a_{Detritus}(676nm, r) \geq 0 \quad (8)$$

$$w_1 a_{Phyto1}(\lambda) \geq w_3 a_{Phyto3}(\lambda) \quad (9)$$

$$w_2 a_{Phyto2}(\lambda) \geq w_3 a_{Phyto3}(\lambda) \quad (10)$$

These assumptions were based on five years of experience in coastal New Jersey waters spanning both the nearshore and offshore. It should be noted that the OSI_m and OSI_c inversion methods using the same assumptions have been successfully used in both the oligotrophic Gulf of Mexico and the southern basin of Lake Michigan (unpublished data). When the OSI method (OSI_m and OSI_c) did not converge on a solution, the data were omitted from the later analysis (<5% of the total New Jersey data set). This generally reflected noise in the ac-9 data most often in near surface waters, presumably

related to air bubbles, which interfered with natural inflections in the absorption curve. Of all the constraints, the requirement that green algae were always less abundant than chlorophyll c and phycobilin containing algae was admittedly the most artificial. However running the inversion without the constraint greatly compromised the efficacy of the inversion for the overall phytoplankton absorption spectra. Omitting the chlorophytic algae also compromised the efficacy of the OSI method (data not shown). Phytoplankton pigment concentrations from discrete measurements during this study confirmed green algae were only a background population of green algae; however green algae were detectable throughout the study (Moline et al. this issue). To assess the stability of the OSI, random noise was introduced into the ac-9 spectra. For this analysis we added $\pm$ 0.005 m^{-1} to the data randomly across all wavelengths. Results indicated that there was no spectral bias and the quantitative impact was less then 1%.

3. Results & Discussion

3.1 Verification of the Derived Optical Products

OSI-derived particulate, detrital and phytoplankton loads were compared to three independent datasets that included stimulated chlorophyll fluorescence, phytoplankton filter pad absorption measurements, and HPLC phytoplankton pigment concentrations. All three data comparisons suggested that the OSI method provided reasonable estimates of particulate, phytoplankton, detritus and CDOM optical weights.

Fluorescence. The ac-9 derived phytoplankton absorption and stimulated *in situ* chlorophyll fluorescence were positively and linearly related to each other (Figure 2). The derived phytoplankton absorption was significantly correlated ($p < 0.05$) with fluorescence and could explain 54% and 61% of the variance in the summers 2000 and

2001 respectively. The linear relationship between the fluorescence and derived phytoplankton weight was notable given that the majority of the data were collected in Case 2 waters where phytoplankton are not necessarily the dominant optical signal (see below). Secondarily a significant proportion of the phytoplankton communities were light-saturated for photosynthesis and thus fluorescence quenching was significant (Falkowski and Kiefer 1985, Figure 3). This quenching contributed to the variance in the correlation between the OSI-derived phytoplankton optical weights and chlorophyll fluorescence measurements. Xanthophyll pigment cycling (Demmig-Adams 1990; Owens et al., 1993) and photoinhibition (Prasil et al. 1992, Nickelsen and Rochaix 1994, Critchley 1994) often results in almost a 100% change in fluorescence quantum efficiency (Falkwoski and Keifer 1985, Kroon 1994). The variable fluorescence quantum yield compromises the accuracy of using fluorescence to estimate chlorophyll a biomass. The OSI phytoplankton estimates may be more desirable then the commonly used chlorophyll fluorometer because it is not subject to physiological variability. IOP sensors are now becoming operationally viable for the wider oceanographic community and inverted optical data will improve our ability for making quantitative biomass maps.

Filter Pad Absorption. The OSI results were compared to 240 filter pad samples that spanned the period of the field effort (Figures 4 and 5). For OSI_m, quantitative agreement with discrete samples for particulates was good with the R^2 ranging from 0.8 to 0.5 for wavelengths lower than 680 nm with least success associated with the wavelengths of carotenoid and phycobilin absorption (530 to 600 nm) (Fig. 4A). The R^2 dropped to 0.3 for wavelengths greater than 680 nm. The average slope between the measured and predicted absorption ranged from 1.2 to 0.5. Given the variance within the

correlations, the average slope was rarely significantly different from one. The OSI_m could account for 70% of the variance in measured phytoplankton spectra except for the wavelengths associated with phycobilin/cartenoid absorption spanning from 530 nm to 580 nm (Fig. 4B). The R^2 dropped for wavelengths greater than 680 nm. Average slopes between measured and predicted phytoplankton absorption were insignificantly different from one except in the low blue wavelengths (< 415 nm) of light where phytoplankton absorption were overestimated by as much 20% (Fig. 4B). OSI-derived detritus spectra could account for 70% of the variance in the absorption in the blue wavelengths of light (Fig. 4C), but the R^2 dropped off at the higher wavelengths due to the low signal to noise associated with the exponential decline in detrital absorption with increasing wavelength. The CDOM absorption was significantly overestimated. In the blue wavelengths, this overestimate was 35% but increased to a factor of 2 in the green orange wavelengths of light (Fig. 4D); however the OSI_m derived CDOM absorption could account 88% of the variance in the measured CDOM absorption in the blue wavelengths of light. Similar to the detritus the R^2 decreased with increasing wavelength due to decreasing signal to noise.

For the OSI_c the quantitative agreement between measured and modeled particulate spectra was good, with the R^2 ranging from 0.5 to 0.9 with low values associated with wavelengths greater than 680 nm (Figure 5A). The slope between the measured and modeled particulate spectra ranged from 1.2 to 0.8 depending on wavelength (Figure 5A) and the variance was reduced from the OSI_m approach especially in the wavelengths associated with phycobilin and carotenoid absorption (530-580 nm). For the majority of the wavelengths, the deviations of the average slope from 1 were

rarely statistically significant (Figure 5A). Quantitative agreement decreased in the red wavelengths of light where signal was low. Results indicate that the derived particulate spectra could be quantitatively derived from the ac-9 with minor spectral biases despite that only idealized spectral absorption shapes were used. The agreement for the OSI and measured phytoplankton spectra were good (Figure 5B). The largest mismatches were in the blue wavelengths of light but 70-80% of the observed variance in the measured spectra were described by the OSI_c and as with the particulate spectra the errors were lower compared to the OSI_m method. Quantitative estimates for detritus were good (Fig. 5C), but accuracy dropped in the higher wavelengths due to low detrital absorption. The OSI_c method showed no improvements over the OSI_m method for predicting CDOM absorption, with the overall CDOM absorption being overestimated significantly (Fig. 5D). For both OSI_m and OSI_c the spectral slope of the CDOM was underestimated especially when discrete samples indicated high slopes (Fig. 6).

In our approach, the input spectra for the OSI were based on laboratory data (Johnsen et al. 1994) and theoretical curves, so the OSI methods could undoubtedly be improved by customizing the input spectra for any particular location. Our goal however was to assess what could be derived using no local input data. The relative particulate spectra derived by the OSI_c approach over-estimated absorption at wavelengths of peak phytoplankton absorption (420-540 and 660-680 nm). This is consistent with the well-documented package effect, where absorption spectra are “flattened” when pigments are packaged within a cell (Morel and Bricaud 1986). The package effect is greatest in the wavelengths of maximal absorption and increases with increasing cell size and cellular concentration of pigment. In higher chlorophyll waters nearshore, water samples

revealed high populations of large net diatoms (Moline et al, 2004), which have been found to be greatly affected by the pigment package effect (Bricaud et al. 1994). Filter pad measurements support the hypothesis that phytoplankton were highly packaged as the specific absorption at 676 nm was consistently lower (0.017 m^2 mg chl$\underline{a}^{-1}$) than in low chlorophyll offshore waters where populations were dominated by picoplankton. Therefore as the majority of the data collected represented nearshore stations, the package effect could account for much of spectral differences in the derived spectra.

The spectral mismatch resulting from the highly peaked phytoplankton contributed to the overestimated CDOM absorption. This is associated with the high pigment absorption in the blue and red wavelengths of light. Given the OSI requirement that phytoplankton dominate the red absorption peak, a flatter phytoplankton input absorption spectra would result in 1) lower the overall CDOM and detrital estimates in the blue wavelengths and 2) steeper estimates in the CDOM exponential slope. This would argue that laboratory spectra should not be used in the inversion of field data; however it was the highly peaked pigment shoulders that allowed phytoplankton community composition to be determined. Until more wavelengths are available to allow researchers characterize both composition and pigment packaging researchers will be forced to prioritize their needs. This shortcoming will improve in the coming years as *in situ* hyperspectral sensors are actively being developed by the community.

Phytoplankton Pigments. To further assess the phytoplankton absorption inversion estimates, we examined how well the presence of the three spectral classes of phytoplankton could be determined (Figure 7). Using accessory pigment data and the ChemTax program (Mackey et al. 1996, Mackey et. al. 1998) we estimated the

proportion of total chlorophyll a associated with the three major spectral classes of phytoplankton. The inverted phytoplankton estimates from the OSI_c method were significantly correlated ($p < 0.00$) with the ChemTax estimates of chlorophyll *c* and phycobilin-containing phytoplankton (Figure 7). There was no success in predicting the distribution of chlorophyll *b*, but this is consistent with the independent findings that they were a minor component of the phytoplankton community at LEO and thus had low contributions to the optical signals (Moline et al. 2004). The OSI_m approach had no success in predicting the phytoplankton community composition.

Overall results from the OSI show that currently available off-the-shelf technology can provide reasonable estimates of the major optical constituents (CDOM, detritus, particles, and phytoplankton) in Case 2 waters. While the precise phytoplankton community composition was difficult to delineate, the most dramatic gradients in phytoplankton composition could be described given constraints that maximized the phytoplankton absorption in the red wavelengths of light. Improving this and similar inversion methods will require spectral resolutions greater than nine wavelengths, ideally, at the wavelengths associated with phytoplankton accessory pigments (Jefferey et al. 1997). Increased spectral resolution would also allow a variety of spectral pattern recognition methods to be applied (Millie et al. 1997, Schofield et al. 1999, Kirkpatrick et al. 2000, Millie et al. 2003), which will increase our ability to discriminate the major spectral classes of phytoplankton and even specific phytoplankton taxa (Millie et al. 2002, Schofield et al. in review). Many of these approaches require spectral resolutions of 2-3 nm (Roelke et al. 1999) so developing hyperspectral instrumentation will be key to improving optical discrimination techniques for coastal waters. Despite shortcomings,

this approach appears very promising as the distributions of the major absorbing components at LEO corresponded to large-scale hydrographic changes (Chang et al. 2002, Johnsen et al. 2003).

3.2 Summer distributions in the optical products

Derived optical products were variable in space and time, as significant differences were observed between the two summer experiments. Optical parameters (discussion from here refers to the OSI_c inverted estimates) showed robust relationships to hydrography, suggesting that the derived optical products reflected natural variability (Figures 9-10).

Summer 2000. In summer 2000, storm events and a low salinity plume dominated the hydrography (Chang et al. 2002, Johnson et al. 2003). The highest concentrations of phytoplankton, CDOM, and detritus were found above the summer thermocline which was found between 7 and 10 m (Figs. 8). Phytoplankton, CDOM, and detritus equally dominated absorption in the blue wavelengths, except in the thermocline, where phytoplankton absorption dominated (Figure 8A), and in offshore bottom waters where CDOM and detritus absorption dominated (Figures 8B and 8C). The net effect is pronounced blue light absorption, and corresponding low blue reflectance leading to the pristine green coastal waters that grace the New Jersey shore. While the relative absorption of phytoplankton, CDOM, and detritus were generally inversely related to each other, the observed variances co-varied spatially with the highest variances observed 15-20 km offshore throughout the water column (Figure8D, 8E, 8F). The variance was highest just offshore of an observed salinity front that was associated with the Hudson River (see Figures 8B and 8C in Chang et al 2002, also see Johnsen et al. 2003). The

offshore side of the front was impacted by a tidally-induced convergence zone (Schofield et al. 2002) that could be delineated with using surface current radar measurements (Chang et al 2002, Schofield et al. 2002). On the incoming tide, material accumulated offshore of the southern flowing jet, which was then dispersed upon reversal of the tide. This convergence/divergence feature was persistent during the experiment to such a degree that it was possible to adaptively sample the feature (Schofield et al. 2002).

Summer 2001. Summer 2001 was dominated by alternating upwelling and downwelling favorable winds that resulted in strong stratification. Phytoplankton distributions (Figure 9A) were highly correlated with temperature (data not shown) and were higher then in summer 2000. Consistent with summer 2000, the optical estimates for CDOM and detritus were highest in surface waters above the 10m thermocline. During this upwelling summer season, phytoplankton concentrations dominated the total absorption in the surface waters above the thermocline. CDOM and detritus absorption were highest in bottom waters (Fig. 9B). In contrast to the CDOM absorption and variance which were highest offshore, the relative detrital absorption was highest in the nearshore bottom waters below the thermocline (Fig. 9C). The variance was highest for all three parameters at the interface between the phytoplankton dominated surface waters and CDOM dominated bottom waters (Figure 9D-F). The alternating onshore and offshore transport of the cold bottom waters transported optically distinct waters into our study site. The total absorption in these cold bottom waters was dominated by CDOM absorption with only minor contributions from phytoplankton or detritus. Detrital absorption was highest in bottom waters, which correlated with discrete measurements that indicated the presence marine snow and transparent exopolymer particles (Alldrege

and Silver, 1988, Alldredge et al. 1993, Passow et al. 1994). This cold offshore water was also delineated by distinct particle types as indicated by the backscattered to total scattered light (b_b/b) ratio. This ratio reflects both the size and the refractive index of the particles (Twardowski et al. 2001, Boss et al. 2003). These waters often contain both re-suspended sediments, which is often a fine-sand\silt mix (Craghan 1995) and/or degraded material from picoplankton-dominated communities found offshore (Moline et al. 2004). The net effect is that both of these variables will increase the b_b/b ratio. Smaller phytoplankton cells have enhanced backscatter due to the size (cf. Mobley 1995) and fine silts tend to have enhanced backscatter cross-sections based on changes in the refractive index (on average 1.05 for phytoplankton to 1.25 for inorganic particles). Offshore bottom waters were consistently delineated by the ratio b_b/b ratio (data not shown) and thus were positively correlated with the CDOM slope.

Delineating Water Masses. Phytoplankton optical loads were positively correlated with the concentration of detritus and CDOM; however no robust predictive empirical relationships could be derived. The positive relationship between CDOM and phytoplankton is consistent with many studies (cf. Nelson and Siegel 2002) but given the proximity to land it was not possible to infer the source of material present. On this shallow continental shelf high frequency wind mixing and numerous upwelling events (Glenn et al. 2004) minimize phytoplankton nutrient limitation allowing for high growth rates. Storm events lead to the resuspension of benthic algal communities into the water column. Finally the local rivers generally have high phytoplankton concentrations. For CDOM, the sources include cellular exudation/lysis/defecation (Kalle 1996, Bricaud et al. 1981, Guixa-Boixeru et al. 1999), resuspension from sediments (Chen 1999, Komada

et al. 2002) and inputs of water ladened with terrestrially derived humics/fulvics (Blough et 1993, Vodacek et al. 1997).

Combining the optical data sets with hydrographic data may assist in differentiating water masses in the MAB (Figure 10). Phytoplankton optical concentrations were in found in water masses where the temperatures ranged from 12 to 25 °C and the salinities ranged from 34 to 27 PSU (Figure 10). This effectively covered the range of hydrographic conditions observed and thus phytoplankton concentration did not show great utility in delineating water masses (Figure 10). The CDOM concentrations were highest when water temperatures ranged from 18 to 25 °C and the salinities ranged from 32 to 26 PSU (Figure 10). Highest values were observed for salinities less the 31 PSU, which were largely associated with surface and buoyant river plumes (Fig. 10, Johnsen et al. 2003). In contrast the highest values of the b_b/b ratio were found in lower water temperatures (10 to 20 °C) associated with cold bottom waters. These optical proxies may provide a means for extending traditional water type identification and water mass analysis into multi-dimensional space (Tomczak 1999, Oliver et al.A). These proxies should only be applied when their transformation rates are slower then process being studied. The rate of change of these inverted optical proxies is on the order days to weeks (Falkowski and Raven 1997, Nelson et al. 1998, Nelson and Seigel 2002, Twardowski et al. 2002). This is a great improvement over fluorometric estimates of biomass, which can change on the time scale of hours, and is currently the instrument of choice for most hydrographic packages. Given this we recommend that IOP sensors be routinely incorporated into standard hydrographic surveys.

4. Conclusions

Inversion of absorption data measured using off the shelf technology is possible and shows great promise. These and similar inversion approaches can be applied to optically complex Case 2 waters. Particulate spectra were derived with great efficacy. Deriving phytoplankton spectra was more difficult but achievable. This will provide the marine ecologist a key technology to map specific phytoplankton taxa over ecologically relevant spatial temporal scales. The absorption during the summer upwelling season in the nearshore waters in the Mid-Atlantic Bight were dominated almost equally ($\pm$10%) by phytoplankton, detritus, and CDOM; however the relative absorption of light in offshore bottom waters was dominated by CDOM. Low salinity river plumes were best delineated by high loads of CDOM. These inverted bio-optical parameters will show utility in delineating waters masses in the nearshore coastal ocean.

Acknowledgements. The support of the National Ocean Partnership Program (N00014-97-1-1019) and the Office of Naval Research COMOP and HyCODE programs (N00014-97-0767, N0014-99-0196, N0014-99-0197) are gratefully acknowledged. The other ONR and NRL supported researchers are acknowledged for their patience, humor, and highly valued partnership. The detailed constructive reviews provided by Grace Chang and Emmanuel Boss greatly improved this manuscript. Finally the continuing support from the great state of New Jersey is acknowledged.

References

Alldredge, A. L., U. Passow, and B. Logan, The abundance and significance of a class of large transparent organic particles in the ocean, *Deep-Sea Res*. 40, 1131-1140, 1993.

Alldredge, A. L.and M. W. Silver, Characteristics, dynamics and significance of marine snow, *Prog. in Oceanogr.*, 20, 41-82, 1988.

Aarup, T., N. Holt and N. K. Højerslev, Optical measurements in the North Sea-Baltic Sea transition zone. II. Water mass classification along the Jutland west coast from salinity and spectral irradiance measurements, *Cont. Shelf. Res.*, 16, 1343-1353, 1996.

Barnard, A. H., W. S. Pegau, and J. R. V. Zaneveld, Global relationships of the inherent optical properties of the oceans, *J. Geophys. Res.*, 103(C11):24,955–24,968, 1998.

Blough, N. V., O. C. Zafririou and J. Bonilla, Optical absorption spectra of waters from the Orinoco River outflow – Terrestrial input of colored organic matter to the Carribean. *J. Geophys. Res*., 98, 2271-2278, 1993.

Boss, E., W. S. Pegau, W. D Gardner, J. R. V Zaneveld, A. H. Barnard, M. S. Twardowski, G. C. Chang, and T. D. Dickey, Spectral particulate attenuation and particle size distribution in the bottom boundary layer of a continental shelf, *J. Geophys. Res.*, 106(C5)9, 509–516, 2001.

Bricaud, A., A. Morel, and L. Prieur, Absorption by dissolved organic matter of the sea (yellow substance) in the UV and visible domains. *Limnol. Oceanogr*., 26, 45-53, 1981.

Bricaud, A. M. Babin, A. Morel and H. Claustre, Variability in the chlorophyll-specific absorption coefficients of natural phytoplankton: Analysis and parameterization. *J. Geophys. Res*. 100: 13,321-13,332, 1995.

Carder, K. L., R. G. Steward, G. R. Harvey and P. B. Ortner, Marine humic and fulvic acids: Their effects on remote sensing of chlorophyll a. *Limnol. Oceanogr*., *34*, 68-81, 1989.

Chang, G. C. and T. D. Dickey, Partitioning *in situ* spectral absorption by use of moored spectral absorption-attenuation meters, *Appl. Opt., 38*, 3876-3887, 1999.

Chang G. C., T. D. Dickey, O. Schofield, A. D. Weidemann, E. Boss, M. A. Moline and S. M. Glenn, Nearshore physical forcing of bio-optical parameters in the New York Bight. *J. Geophys. Res.* 107(C9), doi: 10.1029/2001JC001018, 2002.

Chen, R. F., *In situ* fluorescence of dissolved organic matter in seawater, *Mar. Chem.*, 37, 191-221, 1999.

Craghan, M. Topographic changes and sediment characteristics at a shoreface sand ridge: Beach Haven Ridge, New Jersey, M.S. thesis, Rutgers University, New Brunswick, New Jersey, 1994.

Critchley, C., D1 protein turnover: response to photodamage or regulatory mechanism? In Photoinhibition of Photosynthesis from Molecular mechanisms to the Field. Baker, N. R. and J. R. Bowyer (eds) BIOS Scientific Publ., Oxford, 195-201, 1994.

Cullen, J. J, The deep chlorophyll maximum: comparing profiles of chlorophyll a. *Can. J. Fish. Aquatic Sci*., *39*, 791-03, 1982.

Demmig-Adams, B., Carotenoids and photoprotection: a role for the xanthophyll zeaxanthin, *Biochim. Biophys. Acta*, 1020, 1-24, 1990.

Falkowski, P. G. and D. A. Kiefer, Chlorophyll a fluorescence and phytoplankton: Relationship to photosynthesis and biomass. *J. Plankton Res., 7*, 715-731, 1985.

Falkowski, P. G. and J. A. Raven, Aquatic Photosynthesis, Blackwell Scientific Publishers, Oxford, 375 pp., 1997.

Gallegos, C. L. and P. J. Neale, Partitioning spectral absorption in case 2 waters: Discrimination of dissolved and particulate components. *Applied Opt.* 41, 4220-4233, 2002.

Glenn, S, R. A. Arnone, T. Bergmann, W. P. Bissett, M. Crowley, J. Cullen, J. Gryzmski, D. Haidvogel, J. Kohut, M. A. Moline, M. J. Oliver, C. Orrico, R. Sherrell, T. Song, A. Weidemann, R. Chant, and O. Schofield, The biogeochemical impact of summertime coastal upwelling in the Mid-Atlantic Bight, *J. Geophys. Res.* 2004.

Glenn, S. M., D. B. Haidvogel, O. Schofield, J. F. Grassle, C. J. von Alt, E. R. Levine and D. C. Webb, Coastal predictive skill experiments at the LEO-15 national littoral laboratory, *Sea Tech.*, 39, 63-69, 1998.

Glenn S., T. D. Dickey, B. Parker, and W. Boicourt, Long-term real-time coastal ocean observation networks. *Oceanogr*. 13, 24-34, 2000.

Green, S. A. and N. V. Blough, Optical absorption and fluorescence properties of chromophoric dissolved organic matter in natural waters. *Limnol. Oceanogr*., *39*, 1903-1916, 1994.

Guixa-Boixeru, N., D. Vaque, J. M. Gasol and C. Pedros-Alio, Distribution of viruses and the potential effect on bacterioplankton in an oligotrophic marine system, *Aquat. Microb. Ecol.*, 19, 205-213, 1999.

Helland-Hansen, B., Nogen hydrografiske metoder form. *Skand. Naturf. Mote*., 357-359, 1916.

Højerslev, N. K., N. Holt and T. Aarup, Optical measurements in the North Sea-Baltic Sea transition zone. I. On the origin of the deep water in Kattegat, *Cont. Shelf. Res.*, *16*, 1329-1342, 1996.

Jeffrey, S. W., Mantoura, R. F. C., and S. W. Wright, Phytoplankton Pigments in Oceanography. United Nations Educational, Scientific, and Cultural Organization (UNESCO). Paris, 661 pp., 1997.

Johnson, D. M., J. Miller and O. Schofield, Dynamics and optics of the Hudson River outflow plume. *J. Geophys. Res.* 10.1029/2002JC001485. 1-9, 2003.

Johnsen, G., O. Samset, L. Granskog, E. Sakshaug, *In vivo* absorption characteristics in 10 classes of bloom-forming phytoplankton: Taxonomic characteristics and responses to photoadaptation by means to discriminant and HPLC analysis. *Mar. Ecol. Prog. Ser.*, *105*, 149-157, 1994.

Kalle, K., The problem of the gelbstoff in the sea. Oceanogr. *Mar. Biol. Rev*., *4*, 91-104, 1966.

Kiefer, D. A., Chlorophyll a fluorescence in marine centric diatoms: responses of chloroplasts to light and nutrient stress, *Mar. Biol*., *23*, 39-46, 1973.

Kirk, J. T. O., Light and Photosynthesis in Aquatic Ecosystems. Cambridge University Press, Cambridge, 509 p., 1994.

Kirkpatrick, G., D. F., Millie, M. A., Moline, and O. Schofield, Absorption-based discrimination of phytoplankton species in naturally mixed populations. *Limnol. Oceanogr*., *42*, 467-471, 2000.

Kirkpatrick, G. J., C., Orrico, M. J., Oliver, M. A., Moline, and O. Schofield, Continuous real-time determination of hyperspectral absorption of colored dissolved organic matter. *Appl. Opt.* 42(33), 6564-6568, 2003.

Kishino, M., M. Takahashi, N. Okami and S. Ichimura, Estimation of the spectral absorption coefficients of phytoplankton in the sea, *Bull. Mar. Sci*., *37*, 634-642, 1985.

Komada, T., O. Schofield, O. and C. Reimers, Fluorescence characteristics of organic matter released from coastal sediments during resuspension, *Mar. Chem.* 79, 81-97, 2002.

Kroon, B. M. A., Variability of photosystem II quantum yields and related processes in Chlorella pyrenoidsa (Chlorophyta) acclimated to an oscillating light regime simulating a mixed photic zone. *J. Phycol.* 30, 841-852, 1994.

Mackey, M., D. Mackey, H. Higgins, and S. Wright, S., CHEMTAX - a program for estimating class abundances from chemical markers: application to HPLC measurements of phytoplankton. *Mar. Ecol. Prog. Ser*. 144, 265-283, 1996.

Mackey, M. D., H. W. Higgins, D. J. Mackey, and D. Holdsworth, Algal class abundances in the western equatorial Pacific: estimation from HPLC measurements of chloroplast pigments using CHEMTAX. *Deep-Sea Res*. 45, 1441-1468, 1998.

Millie, D. F., O., Schofield, G. J. Kirkpatrick, G. Johnsen, P. A. Tester, P. A. and B. T. Vinyard, Phytoplankton pigments and absorption spectra as potential 'Biomarkers' for harmful algal blooms: A case study of the Florida red-tide dinoflagellate, Gymnodinium breve. *Limnol. Oceanogr*., *42*, 1240-51, 1997.

Millie, D. F., O. Schofield, G. J. Kirkpatrick, G. Johnsen and T. J. Evens, Using absorbance and fluorescence spectra to discriminate microalgae. *Europ. J. Phycol*. *37*, 313-322, 2003.

Mobley, C. D., Light and Water Radiative Transfer in Natural Waters. Academic Press San Diego, 591 p., 1994.

Moline, M. A., S. Blackwell, R. Chant, M. J. Oliver, T. Bergmann, S. Glenn, and O. Schofield, Episodic physical forcing and the structure of phytoplankton communities in the coastal waters of New Jersey, *J. Geophys. Res*. (submitted), 2004B

Morel, A. and A. Bricaud, Inherent optical properties of algal cells including picoplankton: Theoretical and experimental results. In Photosynthetic Picoplankton. Platt, T., and Li, W. K. W. [Eds] *Can. Bull. Fish. Aquat. Sci*. p. 521-59, 1986.

Nelson, N. B., D. A. Siegel and A. F. Michaels, Seasonal dynamics of colored dissolved organic material in the Sargasso Sea, *Deep-Sea Res.*, 45, 931-957, 1998.

Nelson, N. B. and D. A. Siegel, Chromophoric DOM in the open Ocean, In Biogeochemistry of Marine Dissolved Organic Matter, Elsevier Science, San Diego, p. 547-578, 2002.

Nickelsen J and J. D. Rochaix, Regulation of synthesis of D1 and D2 proteins of photosystem II. In Photoinhibition of Photosynthesis from Molecular mechanisms to the Field. Baker, N. R., Bowyer J. R. (eds) BIOS Scientific Publ. Oxford, pp. 179-190, 1994.

Oliver, M. J., J. T. Kohut, A. J. Irwin, S. M. Glenn, O. Schofield, M. A. Moline and W. P. Bissett, Bioinformatic approaches for objective detection of water masses. *J. Geophys. Res.*, 109, C07S04, doi:10.1029/2003JC002072, 2004a.

Oliver, M. W., O. Schofield, T. Bergmann, S. M. Glenn, M. A. Moline and C., Orrico, *In-situ* optically derived phytoplankton absorption properties in coastal waters and its utility for estimating primary productivity rates. *J. Geophys. Res*., 109, C07S11, doi:10.1029/2002JC001627, 2004b.

Owens, T. G., A. P. Shreve and A. C. Albrecht, Dynamics and mechanism of singlet energy transfer between carotenoids and chlorophylls: light-harvesting and nonphotochemical fluorescence quenching, Research in Photosynthesis Vol. IV, In: Murata, N. [ed.]. Kluwer Academic Publishers, Dordrecht, pp. 179-186, 1993.

Passow, U., A. L. Alldredge, and B. E. Logan, The role of particulate carbohydrate exudates in the flocculation of diatom blooms, *Deep-Sea Res.*, 41, 335-357, 1994.

Pegau, S. W., J. S. Cleveland, W. Doss, D. W. Kennedy, R. A. Maffione, J. L. Mueller, R. Stone, C. C. Trees, A. D. Weidemann, W. H. Wells, and R. J. V. Zaneveld, R. A comparison of methods for the measurement of the absorption coefficient in natural waters. *J. Geophys. Res*., *100*, 13,201-13,221, 1995.

Prasil, O., N. Adir and I. Ohad, Dynamics of Photosystem II: mechanism of photoinhibition and recovery processes. In: The Photosystems: Structure, Function and Molecular Biology. Barber, J. [Ed], Elsevier Publishers, Amsterdam, pp. 295-348, 1992.

Robinson, A. R. and S. Glenn, Adaptive sampling for ocean forecasting, *Naval Res. Rev.* 51, 26-38, 1999.

Roelke, D. L., C. D. Kennedy, A. D. Weidemann, Use of discriminant and fourth-derivative analyses with high-resolution absorption spectra for phytoplankton research: Limitations at varied signal to noise ratio and spectral resolution. *G. Mex. Sci.* 17, 17-28, 1999.

Roesler, C. S., Theoretical and experimental approaches to improve the accuracy of particulate absorption coefficients derived from the quantitative filter technique. *Limnol. Oceanogr., 43*, 1649-1660, 1998.

Roesler, C. S. and M. J. Perry, In situ phytoplankton absorption, fluorescence emission, and particulate backscattering spectra determined from reflectance. *J. Geophys. Res., 100*, 13,279-13,294, 1995.

Roesler, C. S., M. J. Perry, and K. L. Carder, Modeling in situ phytoplankton absorption from total absorption spectra in productive inland marine waters. *Limnol. Oceanogr., 34*, 1510-1523, 1989.

Schofield, O., J. Gryzmski, W. P. Bissett, G. J. Kirkpatrick, D. F Millie, M. A. Moline and C. R. Roesler,. Optical monitoring and forecasting systems for harmful algal blooms: Possibility or pipedream? *J. Phycol. 35*, 125-145, 1999.

Schofield, O., T. Bergmann, W. P. Bisset, F. Grassle, D. Haidvogel, J. Kohut, M. Moline, and S. Glenn, The long term ecosystem observatory: an integrated coastal observatory, *IEEE J. Ocean Engin., 27*, 146-154, 2002.

Schofield, O., J. Boesch, G. Kirkpatrick, J. Kerfoot, M. A. Moline, M. Oliver and W. P. Bissett, Studying Harmful Algal Blooms in a Dynamic Environment: How Can Optics Help The Field-Going Sample-Poor Biologist?, In Application of Optics to Studying Harmful Algal Blooms, M. Babin and J. J. Cullen [Eds], UNESCO, Paris, (In review), 2004.

Tomczak, M., Some historical, theoretical and applied aspects of quantitative water mass analysis, *J. Mar. Res., 57*, 275-303, 1999.

Twardowski, M. S., J. M. Sullivan, P. L. Donaghay, and J. R. V. Zaneveld, Microscale quantification of the absorption by dissolved and particulate material in coastal waters with an ac-9, J. *Atmos. Oceanic Technol.*, 16(6), 691–707, 1999.

Twardowski, M. S, E. Boss, J. B. MacDonald, W. S. Pegau, A. H. Barnard and J. R. V. Zaneveld, A model for estimating bulk refractive index from optical backscattering ratio and implications for understanding particle composition in case I and case II waters. *J. Geophys. Res., 106*, 14,129-12,142, 2001.

Twardowski, M. S. and P. L. Donaghay. 2002. Photobleaching of aquatic dissolved materials: absorption removal, spectral alteration, and their interrelationship. *J. Geophys. Res,* 107(C8), 6.1-6.12, 2002.

Vodacek, A., N. V. Blough, M. D. DeGrandpre, E. T. Peltzer and R. K. Nelson, Seasonal variation of CDOM and DOC in the Middle Atlantic Bight: Terrestrial inputs and photooxidation, *Limnol. Oceannogr.*, *42*, 674-686, 1997.

Wright, S. W., S. W. Jeffrey, R. F. C. Mantoura, C. A. Llewellyn, T. Bjornland, D. Repeta and N. Welschmeyer, Improved HPLC method for the analysis of chlorophylls and carotenoids from marine phytoplankton, *Mar. Ecol. Prog. Ser.*, *77*, 183-196, 1991.

Figure Legends

Figure 1. The input spectra used in the ac-9 inversion. Note that the spectral slopes for the CDOM and detritus were allowed to vary.

Figure 2. The relationship between chlorophyll *a* fluorescence measured with a HOBI Labs hydroscat-6 and the estimated phytoplankton weight during the summers of 2000 and 2001. The phytoplankton weight was inverted from ac-9 data using the OSI_c approach. The R^2 for summer 2000 and 2001 are 0.54 and 0.61 respectively.

Figure 3. The relationship between chlorophyll for fluorescence and the OSIc-derived spectrally weighted absorption for phytoplankton communities at the Optical Profiler. Note that the nonlinearity between phytoplankton absorption and chlorophyll fluorescence measurements occurs in surface waters during periods of light saturation as a result of fluorescence quenching which reflects a lower fluorescence quantum yield. Light saturation was determined with radio-isotope productivity measurements (Oliver et al. 2004B) were made on discrete water samples collected at the Optical Profiler.

Figure 4. Comparison of measured and modeled particulate, phytoplankton, detritus, and CDOM absorption using the minimal constraint OSI method. The measured data represents absorption spectra made for either filter pads or dissolved organics on discrete samples. The modeled data represents the absorption spectra predicted from the inverted from the ac-9 data. Data were pooled for both years and was linearly regressed at each wavelength providing both the slope and R^2 for each wavelength. The absolute

differences between ac-9 derived and filter pad determinations for (A) particulate, (B) phytoplankton, (C) detritus and (D) CDOM absorption are presented. The grey shadow around the slope represents the standard deviation.

Figure 5. Comparison of measured and modeled (A) particulate, (B) phytoplankton, (C) detritus, and (D) CDOM absorption using the OSI_c method. The measured data represents absorption spectra determined from filter pads or discrete samples for colored dissolved organics. Data were pooled for both years and were linearly regressed against measured absorption spectra at each wavelength providing both the slope and R^2 for each wavelength. The grey shadow around the slope represents the standard deviation.

Figure 6. Comparison of CDOM spectral absorption estimated by the OSI_c and measured with a flow through Breve-buster (Kirkpatrick et al. 2003) and on a discrete sample.

Figure 7. Comparison of the amount of phytoplankton absorption and measured chlorophyll a associated with the three major spectral classes of phytoplankton during summers 2000 and 2001. The amount of chlorophyll a associated with each spectral class of phytoplankton was calculated via CHEMtax using the accessory pigment data measured via high performance liquid chromatography. A) Relationship between measured chlorophyll a to the OSI_m and OSI_c procedures. B) The absorption of chlorophyll c containing algae estimated with the OSI_m and the chlorophyll a associated with chromophytic algae. C) The absorption of phycobilin containing algae estimated with the OSI_m and the chlorophyll a associated with phycobilin containing algae. D) The

absorption of chlorophyll c containing algae estimated with the OSI_c and the chlorophyll a associated with chromophytic algae. E) The absorption of phycobilin containing algae estimated with the OSI_c and the chlorophyll a associated with phycobilin containing algae. F) The absorption of chlorophyll b containing algae estimated with the OSI_c and the chlorophyll a associated with chlorophytic containing algae.

Figure 8. The spatial variability in the percent mean absorption at 440 nm for phytoplankton (A), CDOM (B), and detritus (C) during summer 2000. The pooled variances in the percent mean absorption at 440 nm for phytoplankton (D), CDOM (E), and detritus (F) is also presented. Note the scale changes between the figure panels.

Figure 9. The spatial variability in the percent mean absorption at 440 nm for phytoplankton (A), CDOM (B), and detritus (C) during summer 2001. The pooled variances in the percent mean absorption at 440 nm for phytoplankton (D), CDOM (E), and detritus (F) is also presented. Note the scale changes between the figure panels.

Figure 10. The relationship between temperature, salinity, and optical parameters using the combined databases collected during summers of 2000 and 2001 (n>15,000). A) The relationship between phytoplankton optical weight, temperature and salinity. B) The relationship between backscatter to total scattering ratio, temperature, and salinity. C) The relationship between CDOM optical weight, temperature and salinity. The red box outlines the general properties found in bottom waters at the LEO site. Summer 2000 was impacted by heavy rainfall and a large low salinity plume was observed during the

experiment. The orange box outlines the general properties associated with the buoyant plume.

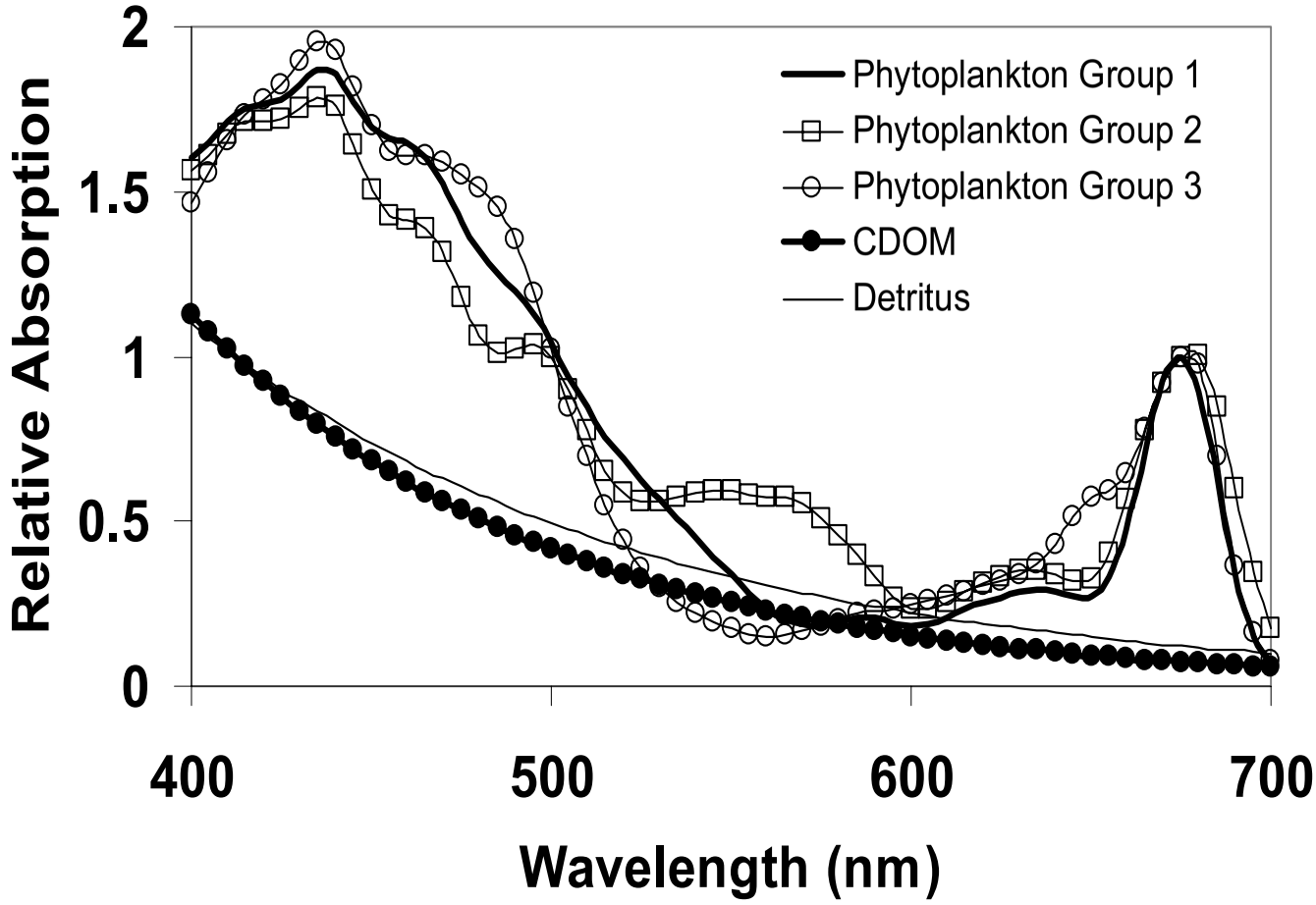
Relative Absorption
2
1.5
1
0.5
0
400
500
600
700
Wavelength (nm)
Phytoplankton Group 1
Phytoplankton Group 2
Phytoplankton Group 3
CDOM
Detritus

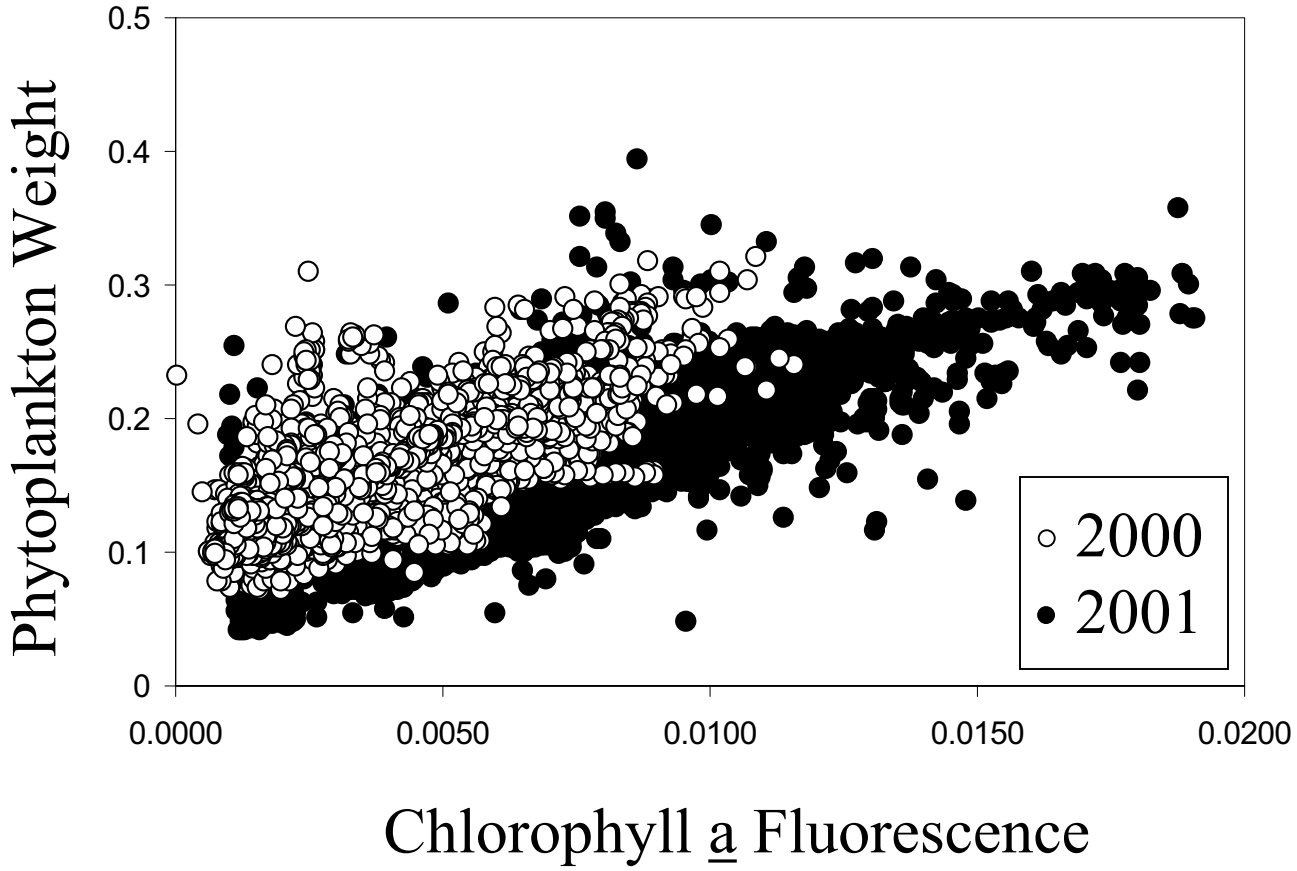
Phytoplankton Weight
0.5
0.4
0.3
0.2
0.1
0
0.0000
0.0050
0.0100
0.0150
0.0200
2000
2001
Chlorophyll a Fluorescence

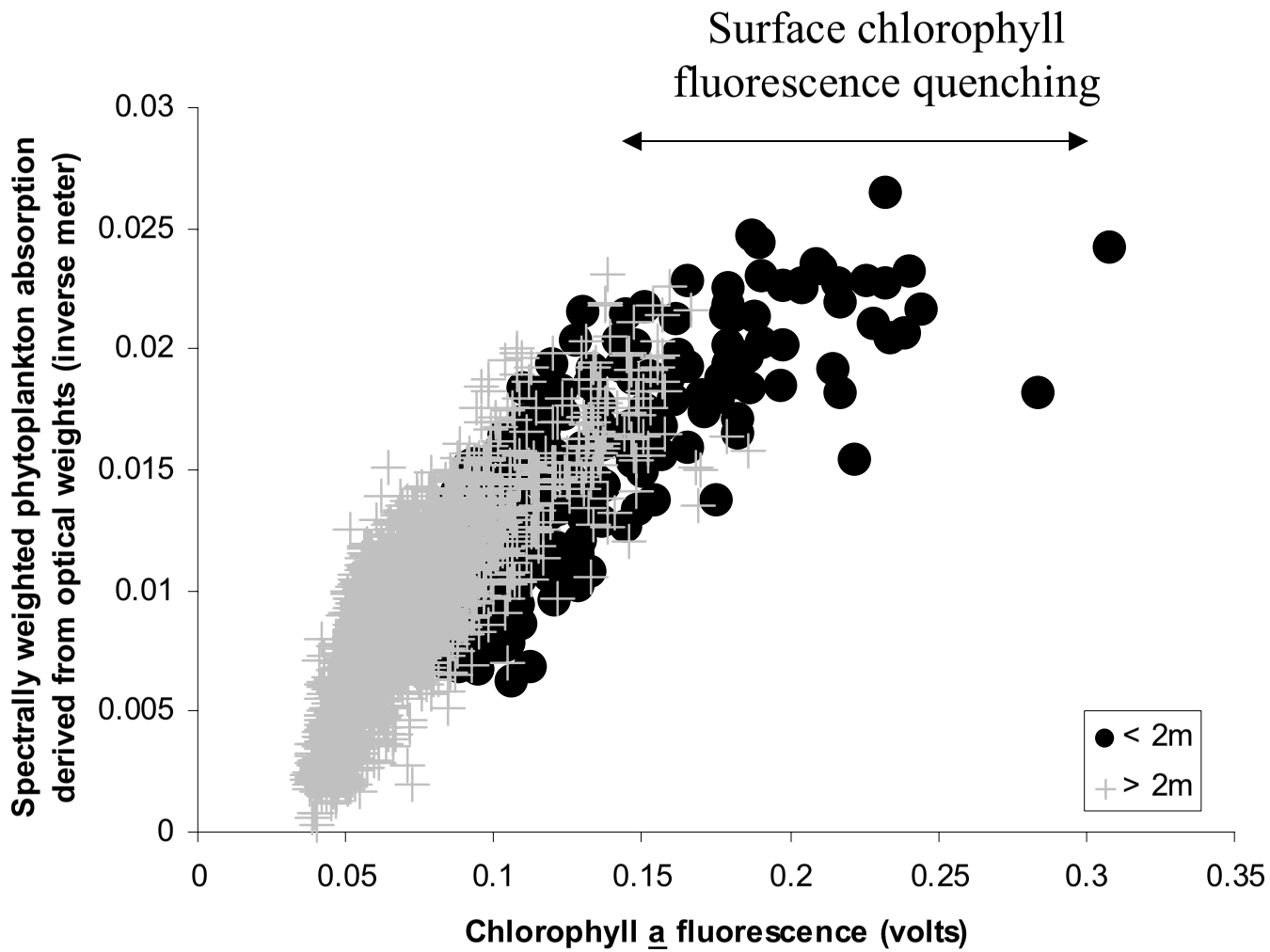
Surface chlorophyll
fluorescence quenching
Spectrally weighted phytoplankton absorption
derived from optical weights (inverse meter)
0.03
0.025
0.02
0.015
0.01
0.005
0
0
0.05
0.1
0.15
0.2
0.25
0.3
0.35
Chlorophyll a fluorescence (volts)
< 2m
> 2m

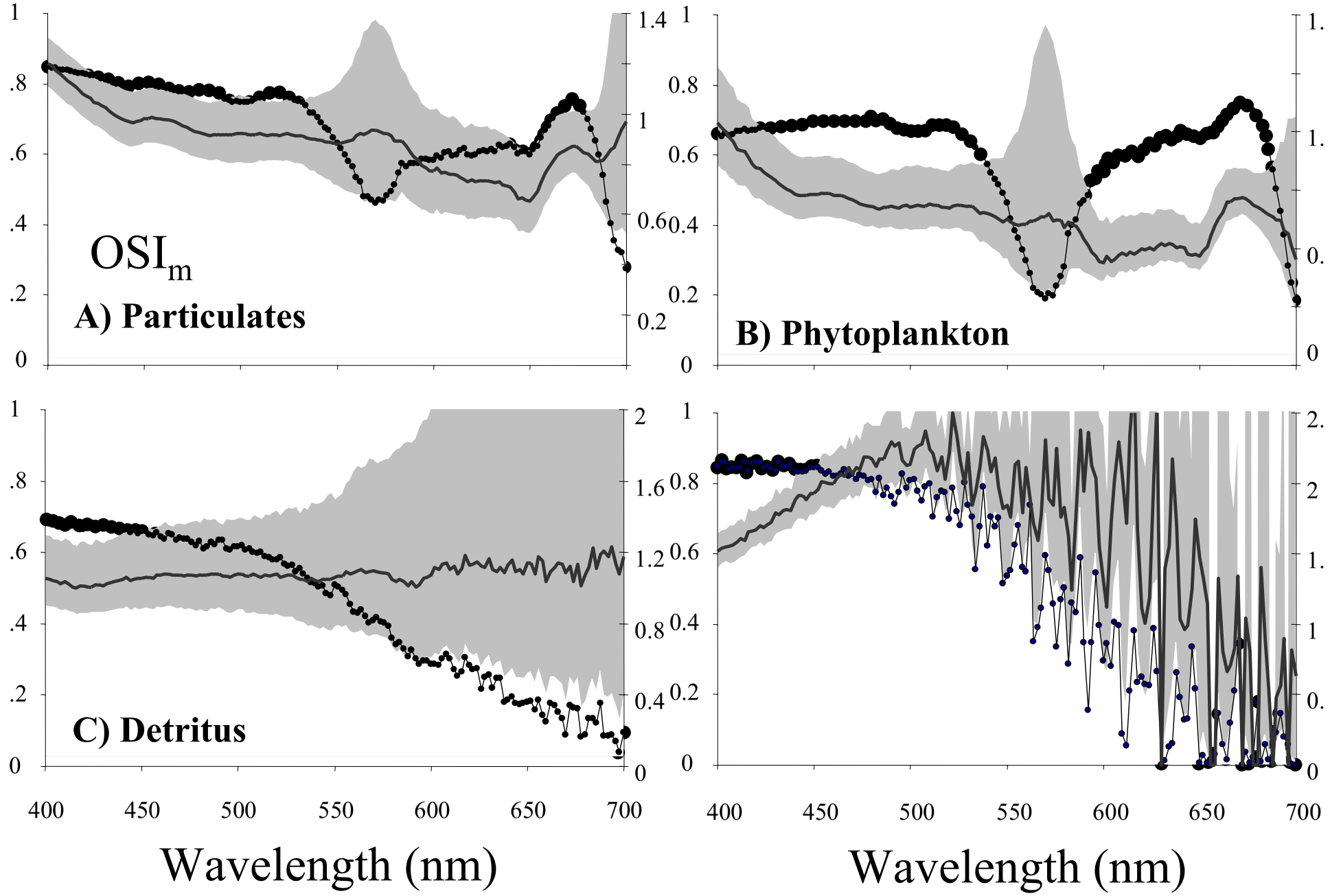
OSI$_m$
A) Particulates
B) Phytoplankton
C) Detritus
Wavelength (nm)
Wavelength (nm)

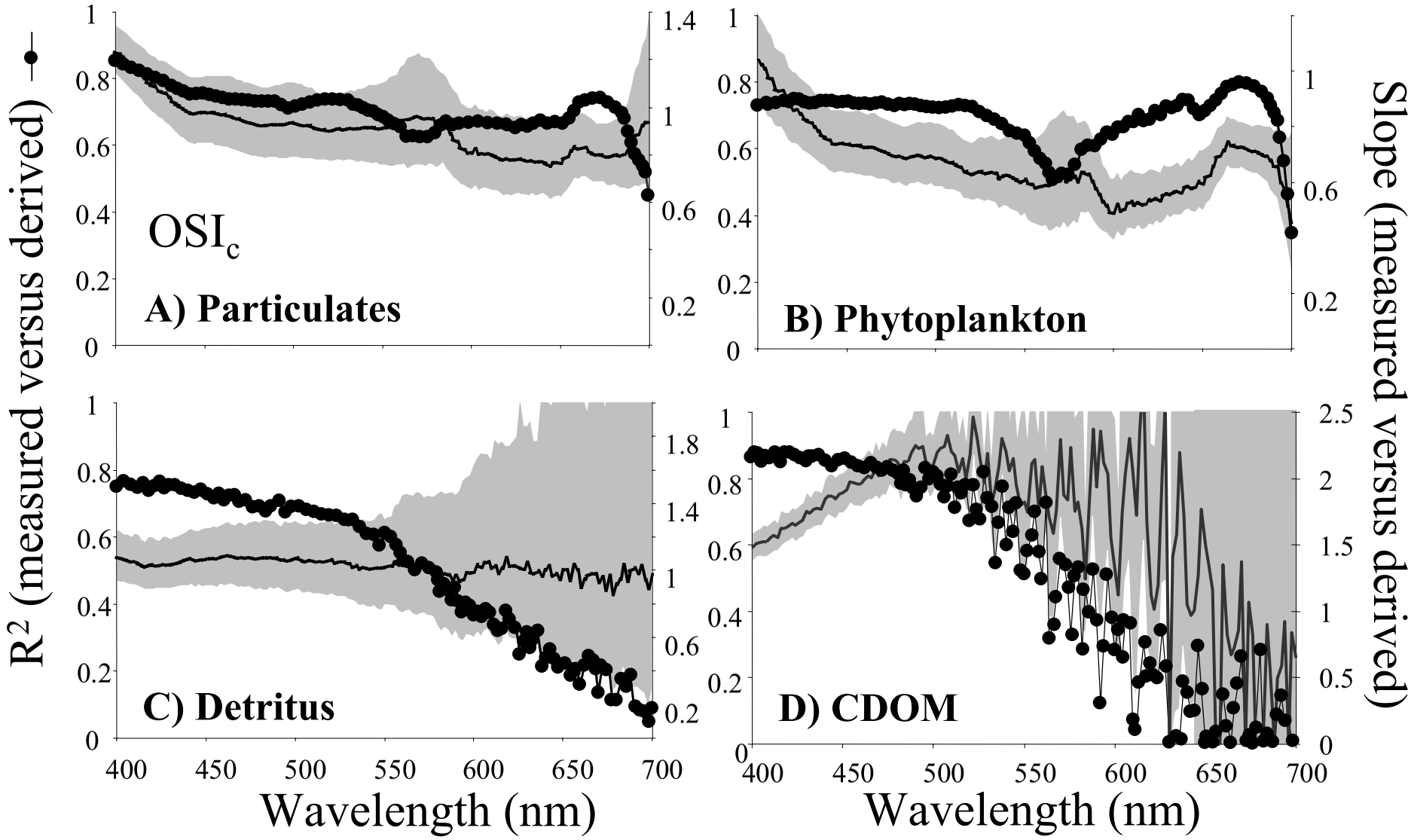
R2 (measured versus derived)
Slope (measured versus derived)
OSIc
A) Particulates
B) Phytoplankton
C) Detritus
D) CDOM
Wavelength (nm)
Wavelength (nm)
400
450
500
550
600
650
700

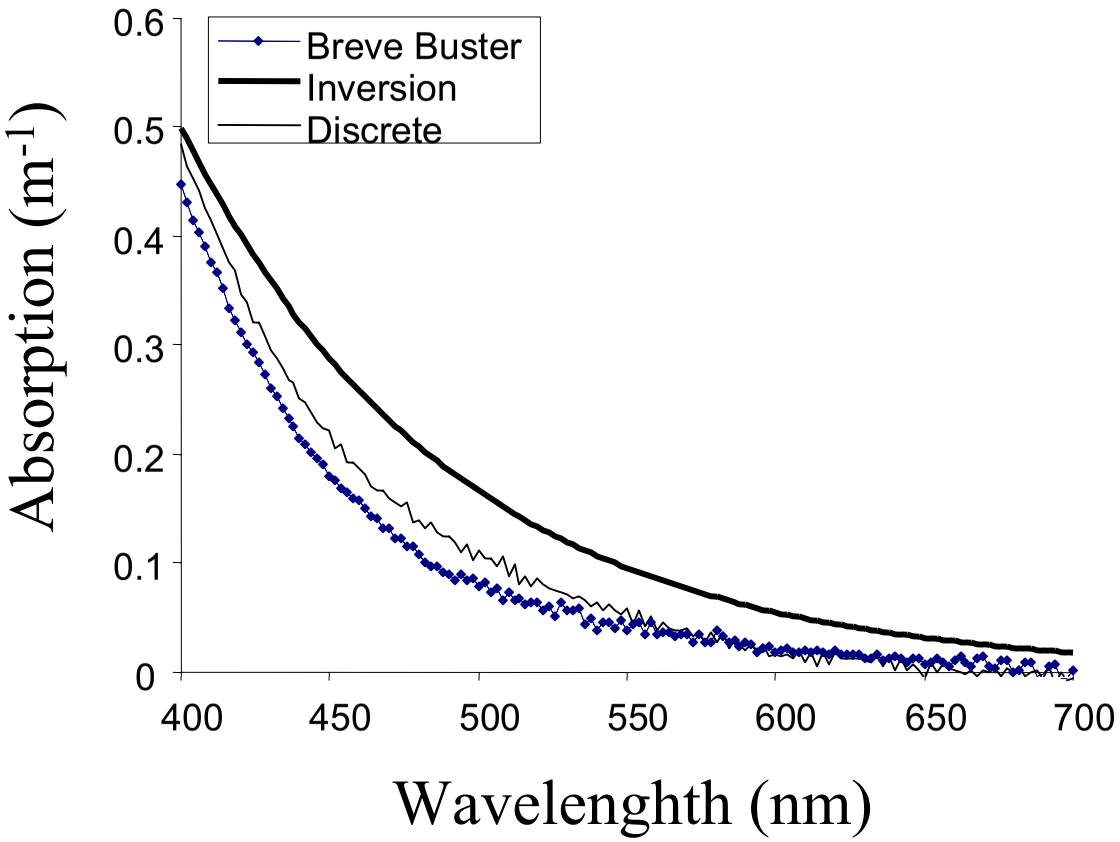
Breve Buster
Inversion
Discrete
Absorption (m-1)
0.6
0.5
0.4
0.3
0.2
0.1
0
400
450
500
550
600
650
700
Wavelenghth (nm)

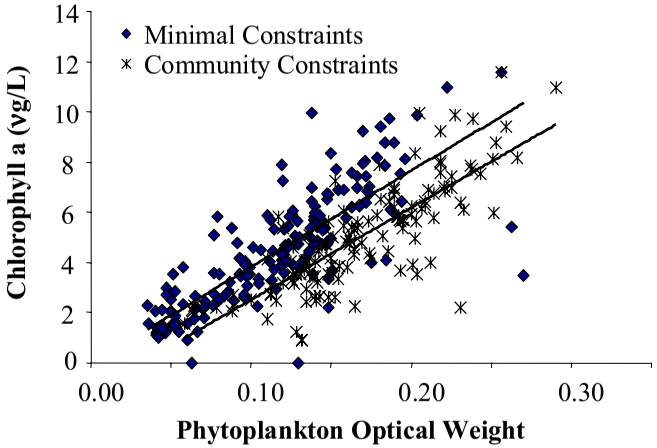
Minimal Constraints
Community Constraints
Chlorophyll a (vg/L)
Phytoplankton Optical Weight
0
2
4
6
8
10
12
14
0.00
0.10
0.20
0.30

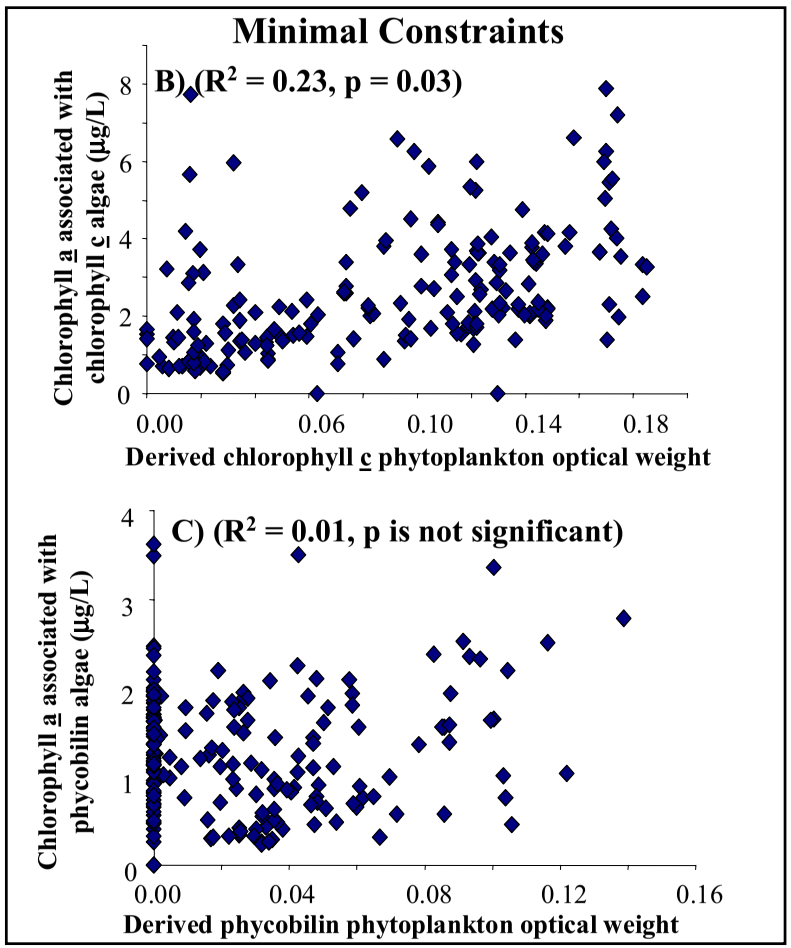
Minimal Constraints
B) (R^2 = 0.23, p = 0.03)
Chlorophyll a associated with chlorophyll c algae (µg/L)
Derived chlorophyll c phytoplankton optical weight
0
2
4
6
8
0.00
0.06
0.10
0.14
0.18
C) (R^2 = 0.01, p is not significant)
Chlorophyll a associated with phycobilin algae (µg/L)
Derived phycobilin phytoplankton optical weight
0
1
2
3
4
0.00
0.04
0.08
0.12
0.16

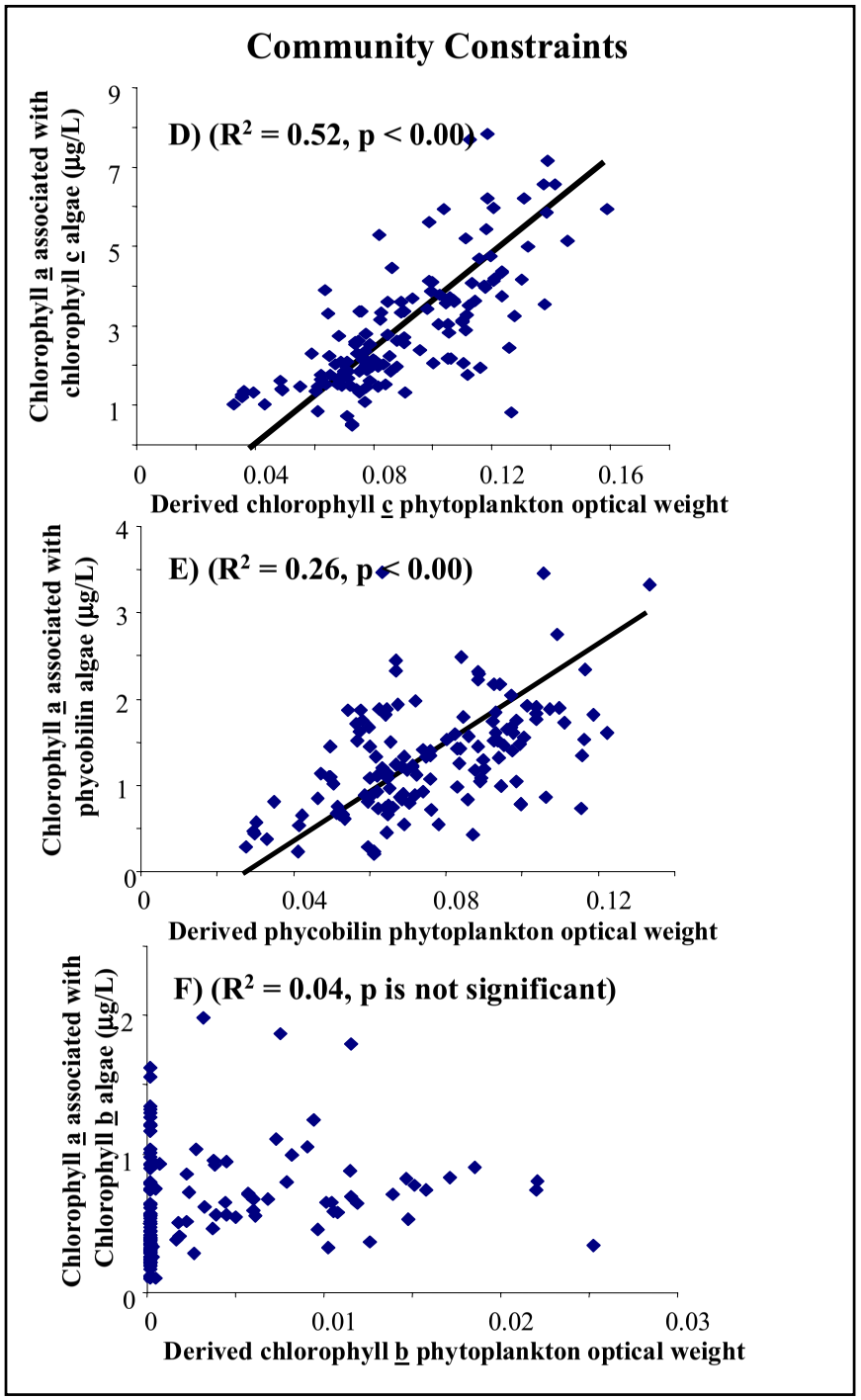
Community Constraints
D) (R^2 = 0.52, p < 0.00)
Chlorophyll a associated with chlorophyll c algae (µg/L)
Derived chlorophyll c phytoplankton optical weight
1
3
5
7
9
0
0.04
0.08
0.12
0.16
E) (R^2 = 0.26, p < 0.00)
Chlorophyll a associated with phycobilin algae (µg/L)
Derived phycobilin phytoplankton optical weight
0
1
2
3
4
0
0.04
0.08
0.12
F) (R^2 = 0.04, p is not significant)
Chlorophyll a associated with Chlorophyll b algae (µg/L)
Derived chlorophyll b phytoplankton optical weight
0
1
2
0
0.01
0.02
0.03

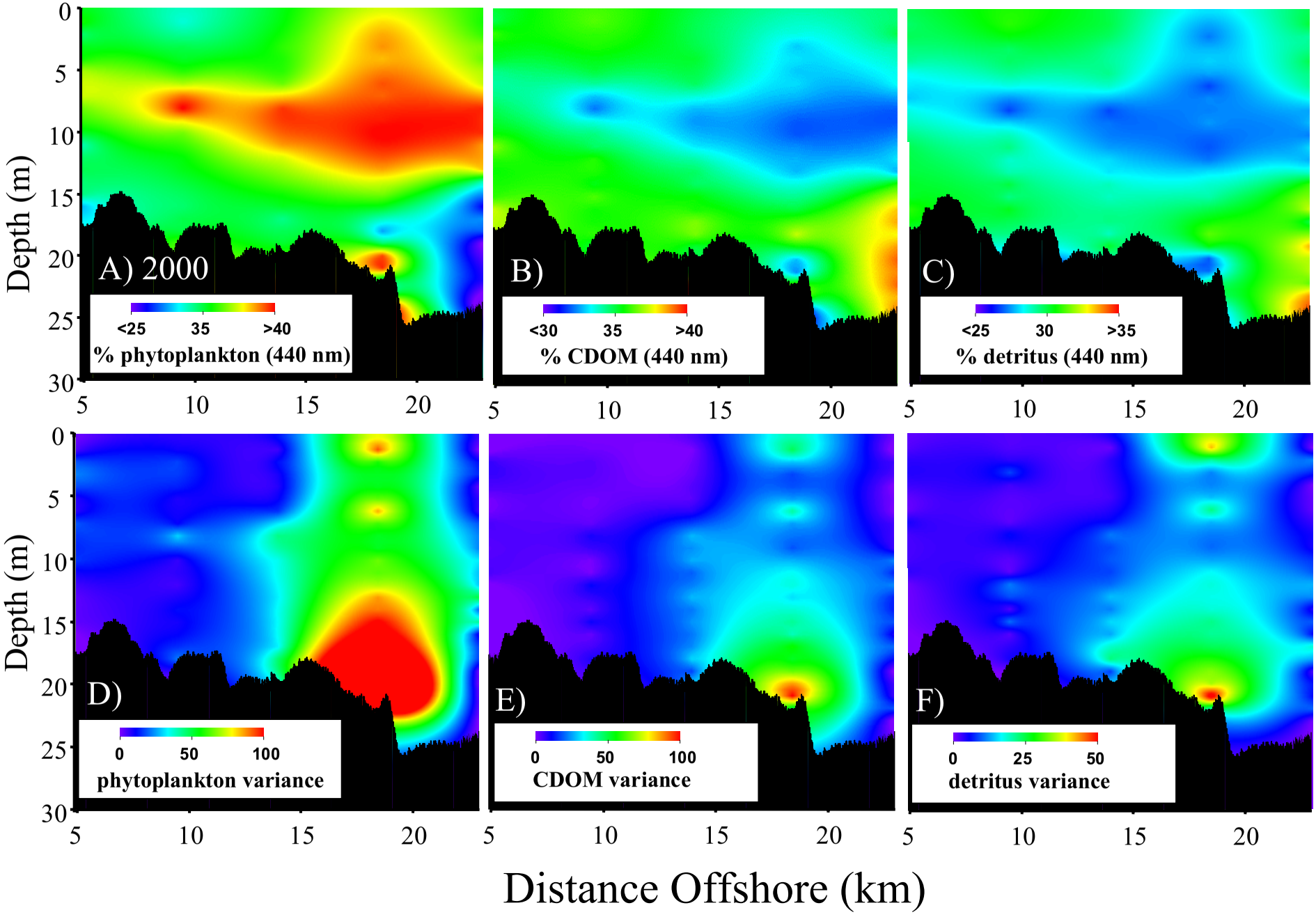
A) 2000
<25 35 >40
% phytoplankton (440 nm)
B)
<30 35 >40
% CDOM (440 nm)
C)
<25 30 >35
% detritus (440 nm)
D)
0 50 100
phytoplankton variance
E)
0 50 100
CDOM variance
F)
0 25 50
detritus variance
Depth (m)
Distance Offshore (km)

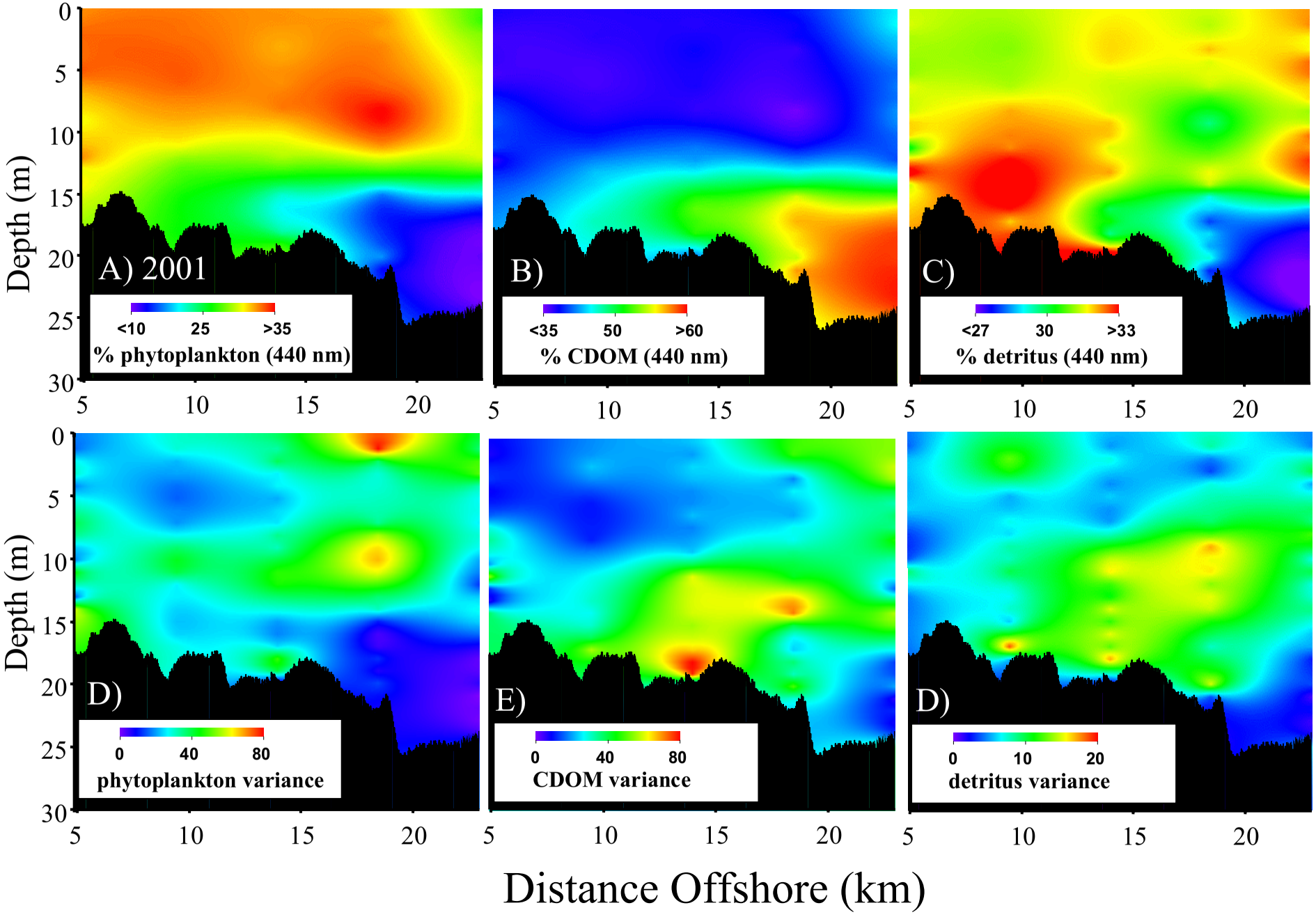
A) 2001
<10 25 >35
% phytoplankton (440 nm)
B)
<35 50 >60
% CDOM (440 nm)
C)
<27 30 >33
% detritus (440 nm)
D)
0 40 80
phytoplankton variance
E)
0 40 80
CDOM variance
D)
0 10 20
detritus variance
Depth (m)
Depth (m)
Distance Offshore (km)

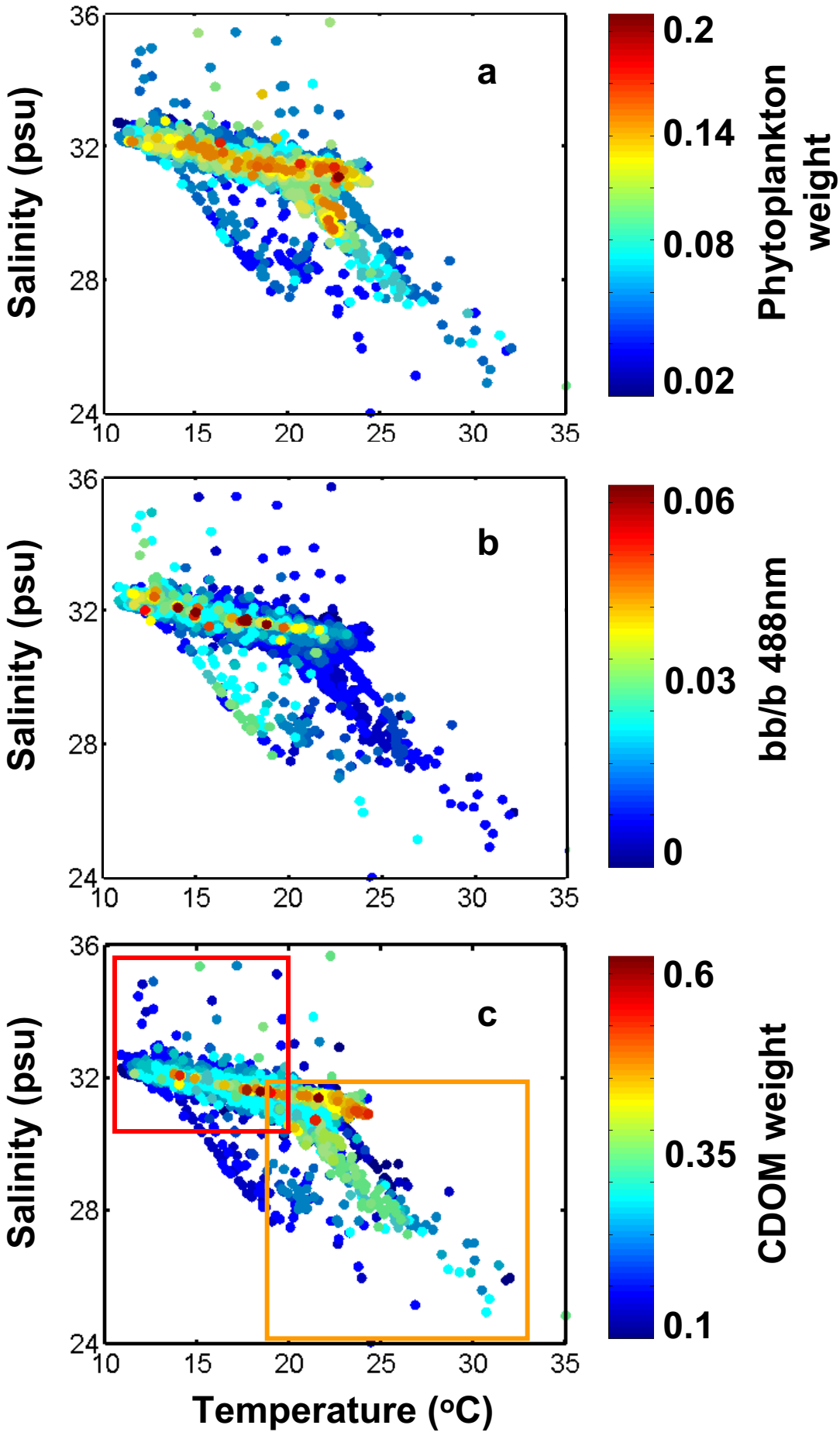
a
b
c
Salinity (psu)
Temperature (°C)
36
32
28
24
10
15
20
25
30
35
0.2
0.14
0.08
0.02
Phytoplankton weight
0.06
0.03
0
bb/b 488nm
0.6
0.35
0.1
CDOM weight